ORIGINAL PAPER

Conceptual model and numerical simulation of the hydrothermal system in Hammam Faraun hot spring, Sinai Peninsula, Egypt

Mohamed Abdel Zaher · Sachio Ehara · Gad El-Qady

Abstract The tectonic position of Egypt in the northeastern corner of the African continent suggests that it may possess significant geothermal resources, especially along its eastern margin. The most of the thermal springs in Egypt are located along the shores of Gulf of Suez and Red Sea. These springs are probably tectonic or nonvolcanic origin associated with the opening of the Red Sea—Gulf of Suez rifts, where the eastern shore of the Gulf of Suez is characterized by superficial thermal manifestations including a cluster of hot springs with varied temperatures. Hammam Faraun area consists of the hottest spring in Egypt where the water temperature is 70°C. Conceptual as well as numerical models were made on the Hammam Faraun hot spring based on geological, geochemical, and geophysical data. The models show that the heat source of the hot spring is probably derived from high heat flow and deep water circulation controlled by faults associated with the opening of the Red Sea and Gulf of Suez rifts.

Keywords Hot springs · Hammam Faraun · Conceptual model · Numerical model · Red Sea · Gulf of Suez

M. A. Zaher · S. Ehara
Laboratory of Geothermics,
Department of Earth Resources Engineering, Faculty of Engineering,
Kyushu University,
744 Motooka, Nishi-ku,
Fukuoka 819-0395, Japan

M. A. Zaher (✉) · G. El-Qady
National Research Institute of Astronomy and Geophysics (NRIAG),
Helwan,
Cairo, Egypt
e-mail: mohamed-zaher@mine.kyushu-u.ac.jp

Introduction

There is a clear correlation between the principal areas of current geothermal development and the seismically active boundaries of the moving segments of lithosphere defined by the plate tectonic models of the earth. It would therefore seem logical to concentrate the search for new geothermal resources along the plate boundaries. The location of Egypt in the northeastern corner of African plate which bounded to the east by what has been interpreted as a median spreading center in the Red Sea (Mckenzie et al. 1970) reflects that this area is an important candidate for geothermal development. Recently, geophysical techniques have been applied intensively in geothermal studies especially in area around Gulf of Suez and Red Sea. These studies show that the most important geothermal resources in Egypt are located on the eastern and western sides of Gulf of Suez, and the hottest one is Hammam Faraun hot spring (Fig. 1). The aim of this study is to construct conceptual model of the hydrothermal system in Hammam Faraun area depending on geological, geochemical, and geophysical data. The features of the conceptual model were reproduced by numerical modeling in order to match the subsurface temperatures and heat flow data in this area.

Geologic regime

The Red Sea and Gulf of Suez occupy part of a large rift valley in the continental crust which was initiated during the late Oligocene to early Miocene by the NE–SW separation of the African and Arabian plates (Patton et al. 1994). This break in the crust is part of a complex rift system that includes the East African Rift System (Said 1962). During this rifting, many faulted tilted blocks were

Fig. 1 Location of the hot springs on the eastern and western sides of the gulf dropped on topographic map of the Gulf of Suez region (from GTOPO30 data set (Gesch et al. 1999))
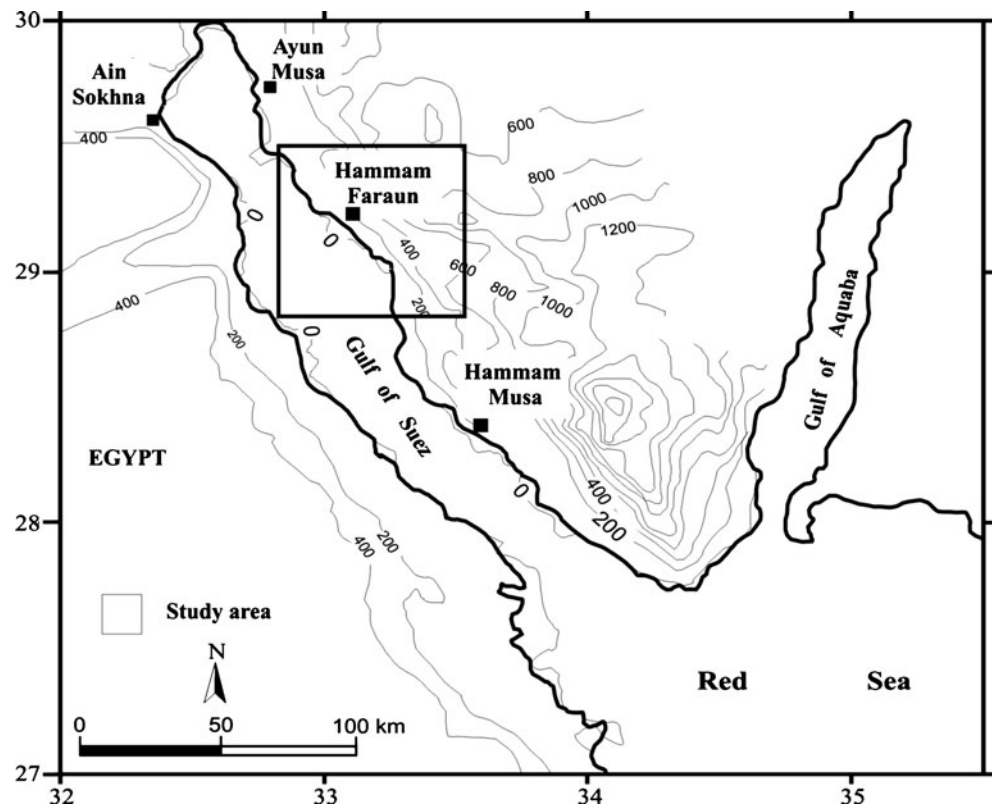
formed, and Hammam Faraun area is one of the main fault blocks in the central west of Sinai Peninsula. The geological map of Hammam Faraun fault block (Fig. 2) shows that this fault block has a half-graben geometry dipping moderately to the east, and it is up to 25 km wide and 40 km long which bounded to the east and west by Thal and Hammam Faraun normal fault zones, respectively. So, the major geological structure feature of this area is a well-defined fault block oriented NW–SE, which is tilted strongly eastward on its western side. The shallow geological succession of Hammam Faraun consists of sand, conglomerate, sandy limestone, lagoonal gypsum limestone, and chalk with flinty limestone.

Materials and methods

Heat in earth's crust represents the greatest potential contribution to the world's energy base. Hence, the target of this study is to draw up the whole picture about the subsurface temperature distribution and heat flow below Hammam Faraun hot spring in order to approach the optimum usage of this hot spring. This was performed based on the obtained geochemical and geophysical data to demonstrate the origin of the thermal water as well as the geological structure setting in the study area. Reprocessing of the geochemical data collected and analyzed by Sturchio et al. (1996) was made to extract more information about

the sources and origin of the thermal water. Furthermore, 2D geoelectrical cross section passing through the hot spring made by El-Qady et al. (2000) gave information about the subsurface geological setting below the hot spring. The purpose of mathematical modeling is to develop a computer model that reflects essential features of the phenomenon considered or represents a real system. A computer model HYDROTHERM version 2.2, 3D finite difference model, is used to simulate groundwater flow and heat transport in porous medium below Hammam Faraun hot spring. The governing equations are expression of mass and energy conservation that are posed in terms of pressure and enthalpy. The mass conservation equation is defined as:

$$[\varphi\rho_1]\frac{\partial}{\partial t} - \nabla\frac{\overline{\overline{K}}K_{rw}\rho_w}{\mu_w}(\nabla P - \rho_w g\nabla z) - Q_m = 0 \qquad (1)$$

And the energy conservation equation is defined by:

$$[\varphi\rho_1 h_1 + (1-\varphi)\rho_m h_m]\frac{\partial}{\partial t} - \nabla\frac{\overline{\overline{K}}K_{rw}\rho_w}{\mu_w}(\nabla P - \rho_w g\nabla z) - Q_h = 0 \qquad (2)$$

Where

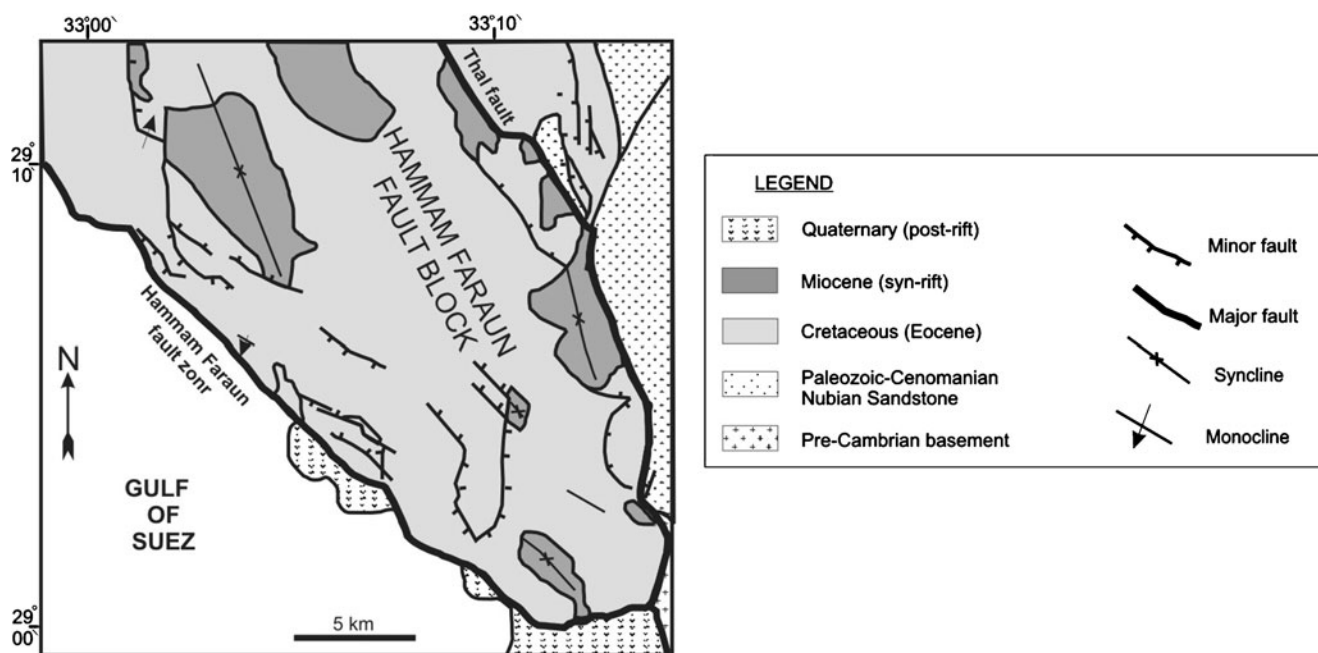|	
Ø	is the porosity
ρ_1, ρ_m, and ρ_w	are the density of the liquid, mass, and water, respectively
K_m	is thermal conductivity

Fig. 2 Geological map of the study area shows that Hammam Faraun region represents a faulted tilted block has a half-graben geometry dipping moderately to the east (after Moustafa and Abdeen 1992; Sharp et al. 2000)

$\overline{\overline{K}}$	is intrinsic permeability tensor
K_{rw}	is relative permeability to liquid water
h_m	is enthalpy
μ_w	is the viscosity of water, and
Q	is a source (+) or sink (−) of solute.

Analytical solutions of these two problems do have a limited applicability, because heterogeneity and multidi-mensionality are reality and additionally, the real world models do have complex constraints which cannot be reflected in analytical solutions. Conversely, the numerical solution of complex nonlinear partial differential equations became possible. Equations 1 and 2 alone are not sufficient to describe a geothermal system. Further constitutive relations are required, and appropriate boundary conditions must be specified. The final product of the modeling

Table 1 Chemical data for Gulf of Suez thermal waters, concentrations in milligram per liter

	Ain Sokhna	Ayun Musa	Hammam Faraoun	Hammam Musa
T, °C	32	37	70	48
pH	7.74	6.02	7.44	7.59
SiO_2	19.1	17.8	51.1	21.6
B	0.04	0.90	0.18	0.04
Li	0.11	0.09	0.32	0.12
Na	1,946	652	3,642	1,586
K	72.2	38.9	127	64.2
Mg	258	52.2	270	330
Ca	413	224	966	523
Sr	16.3	4.85	21.9	10.1
HCO_3	200	243	109	116
SO_4	1,320	378	780	1,130
F	2.4	6.6	2.5	1.6
Cl	3,710	983	8,050	3,870
Br	14	6.3	46	31
T.D.S	7,960	2,600	14,030	7,670
$^{87}Sr/^{86}Sr$	0.70803	0.70776	0.70795	0.70795
$^{3}He/^{4}He$, R_{atm}	–	–	0.256	–

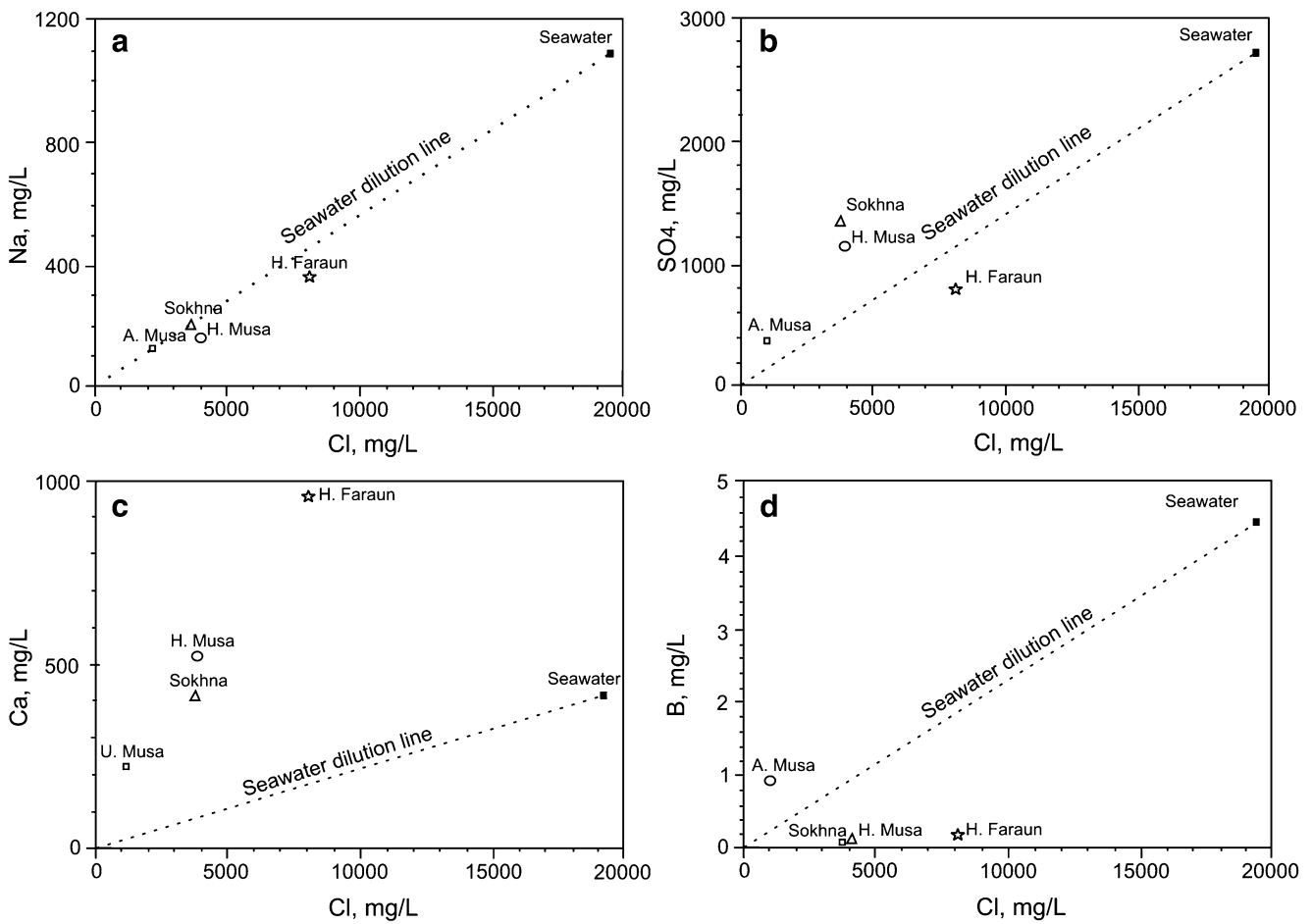Samples collected January 1993 except Ayun Musa, March 1994 (Sturchio et al. 1996)

Fig. 3 Chloride variation diagrams (milligram per liter) for Gulf of Suez thermal waters compared with seawater dilution line (*dashed line*)
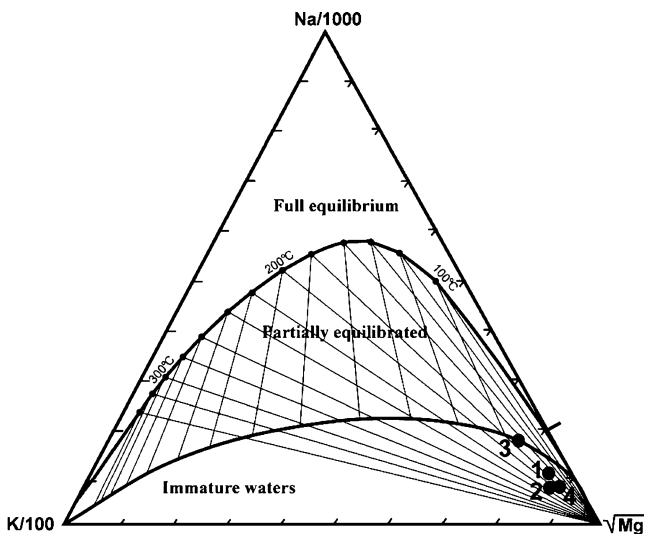
process is a computer model that includes all simplifications and assumptions made at the conceptual model.

Hot water chemistry

Chemical and isotopic analyses of thermal waters of the main hot springs in the areas around Gulf of Suez were made by Sturchio et al. (1996). The studied areas including Ain Sokhna hot spring in the northwestern corner of the

Fig. 4 Ternary diagram of the water–rock equilibration temperatures as modified from Giggenbach (1988) using relative Na, K, and Mg concentrations of the Gulf of Suez thermal waters. *1* Ain Sokhna, *2* Ayun Musa, *3* Hammam Faraun, *4* Hammam Mussa

Table 2 Estimated temperature of the thermal water in Hammam Faraun hot spring by using various types of geothermometers

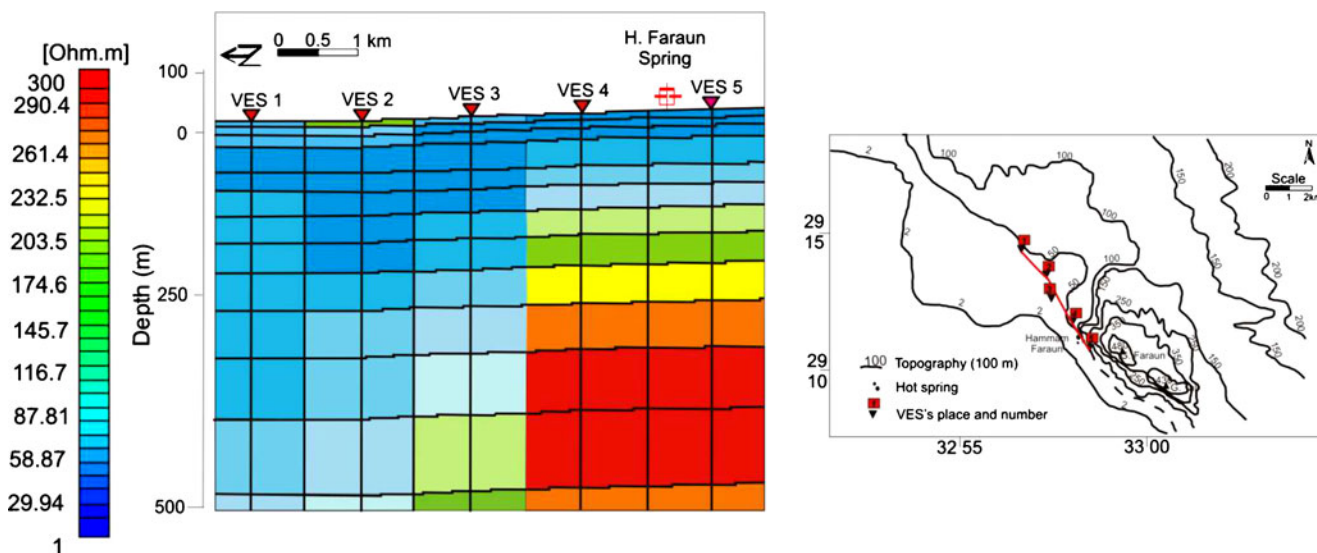| Geothermometers	Estimated temperature (°C)
Emergence temperature	70
CCG (Nieva and Nieva 1987)	128.29
Na–K (Fournier and Truesdell 1973)	140.7
Na–K–Ca (Fournier and Truesdell 1973)	91.53
Silica (Verma 2000)	97.55

Fig. 5 Geoelectric cross section constructed by El-Qady et al. (2000), with the topographic map of the study area shows the location of VESs

Gulf of Suez and Ayun Musa, Hammam Faraun, and Hammam Musa hot springs in the eastern side of the Gulf. Results of chemical and isotopic analyses of thermal waters are presented in Table 1. The most abundant solutes in all thermal waters are Na and Cl, while Mg, Ca, and SO_4 also are prominent, and the pH values are near neutral. The total dissolved solids range from 2,600 to 14,000 mg/l. Generally, chemical compositions indicate derivation of solutes mainly from regional marine sedimentary rocks and windblown deposits (marine aerosol and evaporate dust). Chloride variation diagrams for Gulf of Suez thermal waters were made and compared with the seawater dilution line to provide insight into the origin of these thermal waters. Figure 3a shows the relation between Na and Cl concentrations in milligrams based on the chemical analysis in Table 1. The solutes concentration plotted below the seawater dilution line reflect that some loses of Na ore adding Cl may have been caused by water–rock interaction

within the reservoir. The thermal waters are also enriched in SO_4 relative to the seawater dilution line (Fig. 3b)—except Hammam Faraun hot water due to the derivation of Ca from the dissolution of gypsum in these areas. Figure 3c shows the enrichment of Ca in all thermal waters, and the maximum percentage is recorded in Hammam Faraun hot spring, which implies dissolution of Ca minerals such as calcite and gypsum from surrounding and overlying upper Cretaceous and Eocene carbonate rocks. Almost all thermal waters have low concentrations of boron (Fig. 3d), and this depletion may argue against direct seawater mixing in these areas. However, Boron can adsorb from groundwater onto clay minerals (Palmer et al. 1987).

Additionally, the ratio of 3He/4He was recorded to be 0.256 R_{atm} in the gases emitted from Hammam Faraun hot spring. This ratio indicates that there are excess of helium (3.2%) may be attributed to a deeper source of mantle which represents eight times of the atmospheric ratio (R_{atm};

Fig. 6 Schematic diagram show the conceptual model of the hydrothermal system in Hammam Faraun hot spring area
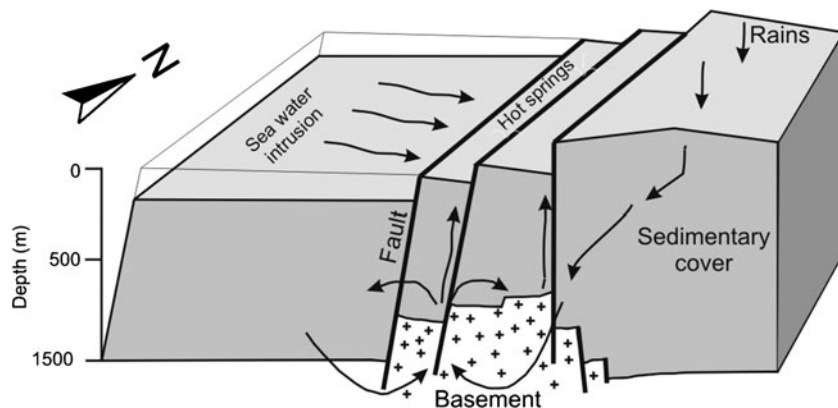
Sano et al. 1988). Sturchio et al. (1996) related such mantle He to the alteration in the subsurface due to late Tertiary volcanic eruptions.

A further evaluation of the cation geothermometers is made on the Na–K–Mg diagram proposed by Giggenbach (1988). Figure 4 shows that none of the Gulf of Suez thermal waters attain a water–rock chemical equilibrium, which indicates a partial equilibrium with the host rock and a possible mixing of different water types (Barragán et al. 2001). Hammam Faraun hot spring is the only water located close to the boundary between mature (partly equilibrated) and immature waters; therefore, temperature estimation by geothermometers can be performed with some degree of confidence.

Chemical geothermometers were applied to the thermal water of Hammam Faraun hot spring, and the results are given in Table 2. The reservoir temperatures computed from the cation geothermometers are generally higher than those of silica geothermometers, this could be explained by silica precipitation due to a cooling and boiling phenomena. It is obvious that Na–K geothermometers give anomalously high temperatures and suggest a deeper reservoir. The Na–K–Ca geothermometer-measured temperatures are lower than those measured by cationic composition geothermometer (CCG), which is due to slightly high Mg contents in the sample. The Mg levels in high temperature geothermal fluids are usually very low (0.01 to 0.1 mg/L; Nicholson
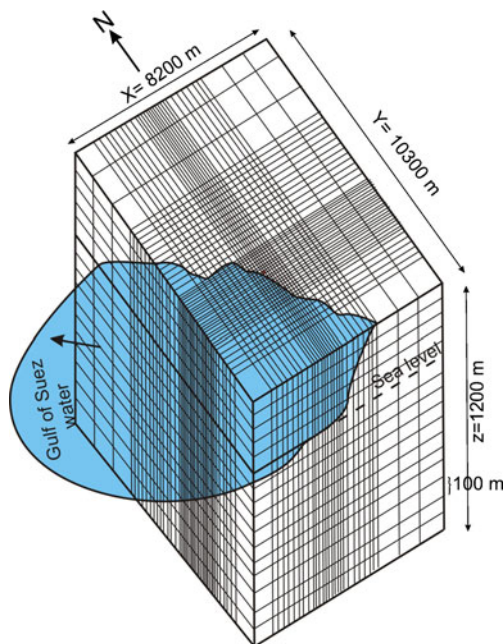

Fig. 8 Plan view of the finite difference blocks for the hydrothermal model on the study area with a total area of 8,200×10,300 m². A simplified topography of Hammam Faraun tilted block as constructed on the model design

1993). The high Mg concentrations in Hammam Faraun hot spring can indicate near-surface reactions that leach Mg from the local rock or dilution by Mg-rich groundwater (Nicholson 1993). The maximum reservoir temperature for Hammam Faraun was obtained by Na/K geothermometer (140.7°C) which represents the temperature of the geothermal reservoir in the study area.

Geophysical studies

El-Qady et al. (2000) used geoelectric resistivity method for detecting and delineating geothermal reservoir and groundwater aquifer at Hammam Faraun area using Schlumberger array of 17 vertical electrical sounding (VES) with maximum AB/2 equal 1,000 m. According to the results obtained through inversion processes, El-Qady constructed 2D geoelectrical cross section for profile parallel to gulf coast and passing through the hot spring (Fig. 5). The general features of the inverted section is a huge thick low resistive body in the northern part of the profile, this correlated with the sea water intrusion in that area. In the southern part, below the hot spring, a high resistive body recognized which may be due to the presence of uplift in basement rock, and this gives a suggestion and explanation for the origin of the hot water at Hammam Faraun hot spring. From that section, we can recognize that there are two structure-faulting systems in NNW–SSE and EW directions affecting the area.

Fig. 7 3D finite difference blocks for the geothermal numerical model on Hammam Faraun area oriented in the N–S direction and divided into 31 blocks in X direction and 43 blocks in Y direction with different size from 100 m at the area of hot spring, up to 1,200 m in the buffering area
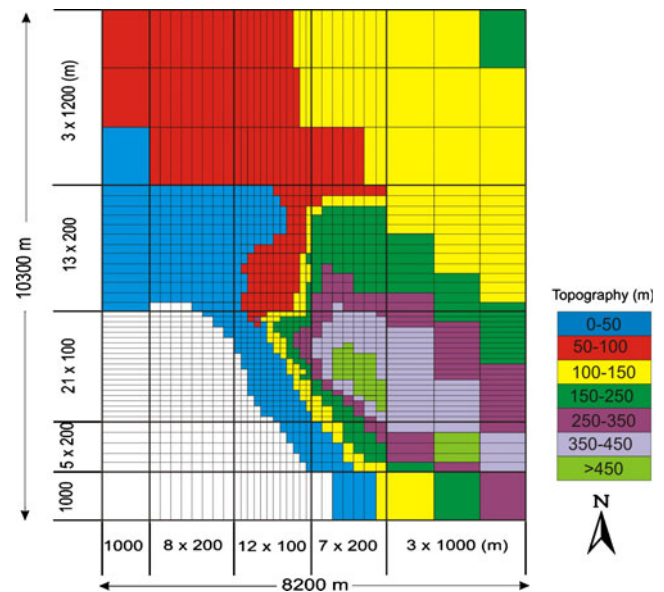
Table 3 Physical rock properties of each layer for the hydrothermal model

	Density (gm/cm^3)	Porosity %	Permeability (Mdarcy)	Thermal conductivity (W/m_k)	Heat capacity (J/Kg.K)
Layer (1)	2.4	10	1	2.4	920
Layer (2)	2.5	5	0.1	1.3	880
Layer (3)	2.4	15	1	2.4	920
Layer (4)	2.67	1.5	0.001	3.0	790
Fracture	1.5	30	100	0.5	1,000

Fig. 9 The E–W temperature distribution and water velocity pattern for slice no. 19 on Hammam Faraun hot spring for steady state condition
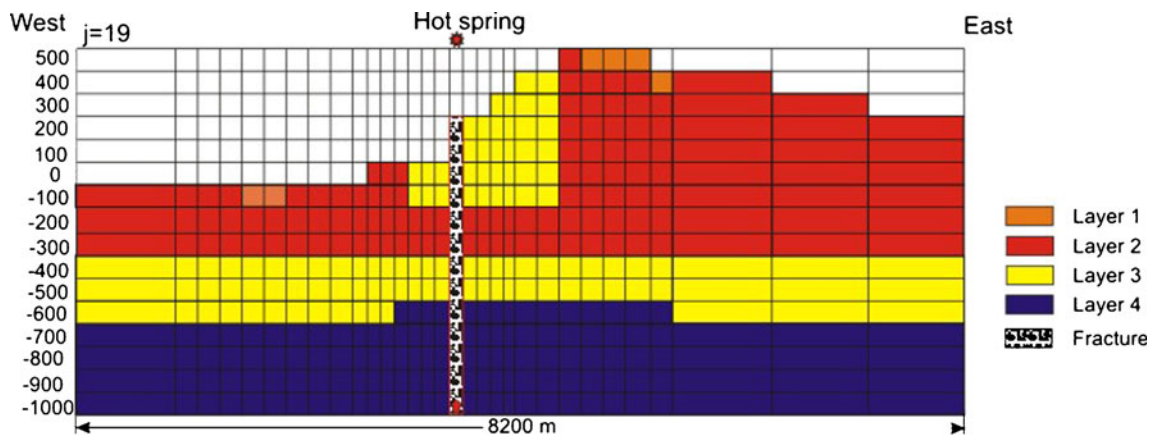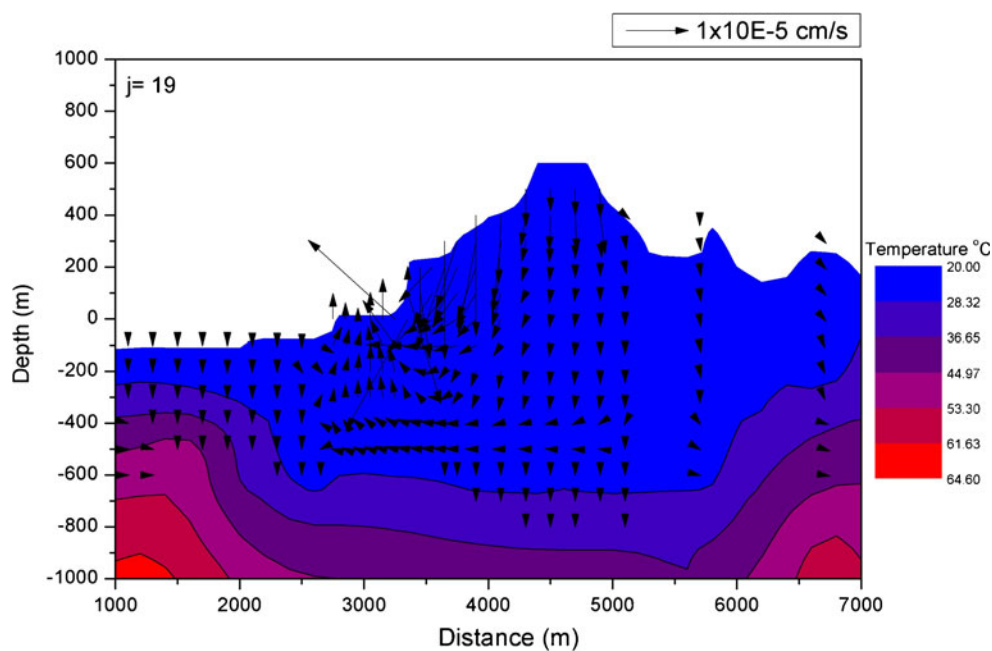

Fig. 10 E–W slice shows the subsurface strata in Hammam Faraun hot spring region including the fracture and heat source below it
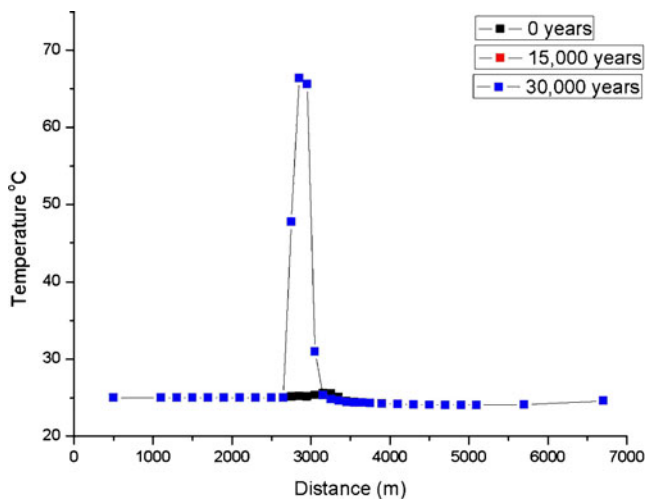
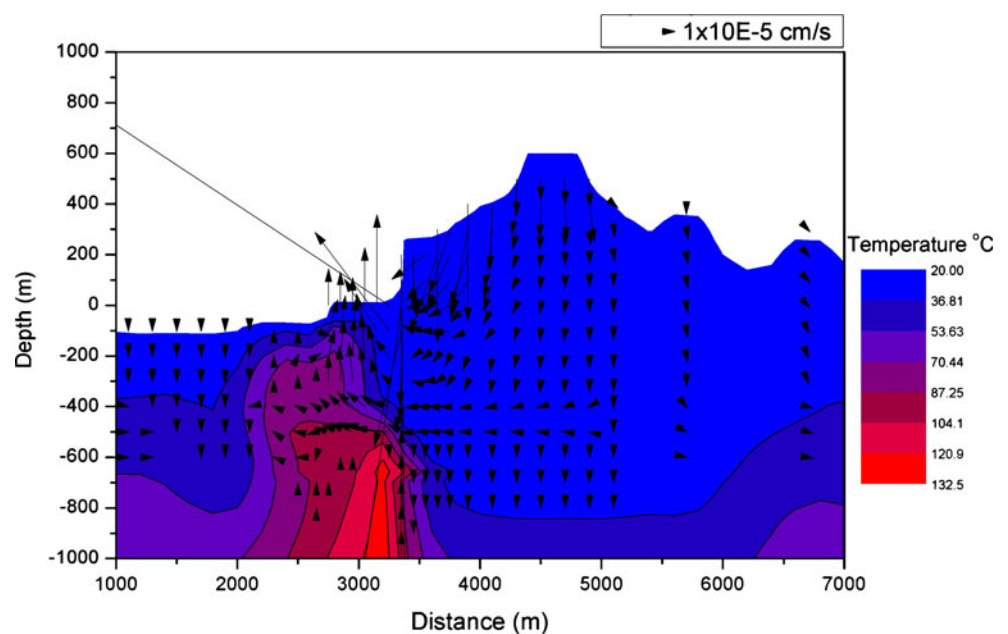Fig. 11 The change in temperature along the upper boundary of slice no. 19 for several simulation times

of the basement rock. The hot water flows upward through vertical fractures and faults parallel to the Gulf of Suez margin. Results of geochemical analyses of thermal water at Hammam Faraun hot spring indicate that the recharge of the deep water comes from meteoric water with minor intrusion of sea water.

Geothermal numerical model

The objectives of the numerical modeling are to match the subsurface temperatures and to reproduce all the significant features of the conceptual model. The numerical simulation model of Hammam Faraun hot spring is considered a total area of 84 km^2. The model was oriented in the N–S direction and divided into 31 slices in X direction and 43 slices in Y direction with different interval size from 100 m at the area under focusing around Hammam Faraun hot springs to more than 1,000 m in the buffered area. Also, the blocks in Z direction were 16 slices with fixed interval size equals 100 m (Fig. 7).

From the topographic and geological information of the area, there are mainly three lithological rock units (alluvial deposits, dolomitic limestone, and sandstone) in addition to the basement rock which is mainly granites. The topography ranges from 0 to more than 450 m (Fig. 8). Table 3 shows the physical parameters using for both the steady state and fracture state. These values consider the main parameters for whole Egypt and were collected from different previous work and various literatures such as El-Nouby and Gaber (2007), El Ramly (1969), Meneisy (1990), and Morgan et al. (1983).

Geothermal conceptual model

Temperature measurements made by Morgan et al. (1985) in the study area show that the temperature in Hammam Faraun area increases with depth by 48 mk/m. The measured temperature gradient is moderately high and reflects that this area is the most interesting for geothermal studies. By using the results from geochemical and geophysical data, conceptual model was made for the geothermal system in Hammam Faraun hot spring (Fig. 6). This conceptual model reflects that Hammam Faraun hydrothermal system is considered dynamic type, and the source of hot spring is due to tectonic uplift of hotter rocks causing deep fluid circulation through faults on the surface

Fig. 12 The E–W temperature distribution and water velocity pattern for slice no. 19 for fracture state

The steady state (nonfracture) simulation was made in order to show the physical characteristic of Hammam Faraun area without any underground heat sources. Therefore, the pressure and temperature were fixed at the upper and lateral boundaries of the lithological units. The ground surface boundary pressure value was specified at 1.013 bars where the ground temperature was fixed at 25°C. The calculated time for simulations is up to 100,000 years. The result of the simulation shows a homogeneous distribution of the subsurface temperature (Fig. 9).

The output temperature and pressure distribution from the steady-state simulation were used as initial conditions for the construction of fracture state model. In this model a heat source is assumed to be located below Hammam Faraun hot spring caused by uplifting of basement rock in this area. The subsurface temperature estimated by the Na/K geothermometer is 140.7°C, which represent the temperature of the geothermal reservoir in the study area. The heat flow upward from the basement rock through fractures and faults affected the whole strata (Fig. 10). Subsurface circulation of geothermal fluids through granitic fractured reservoir leads to chemical reaction and mineral dissolution and precipitation affect the fracture porosity and permeability causing the estimation of these values becomes very difficult. So, by applied different value of fracture permeability in the simulation model, we found that to reach steady state and to get a real simulation model the fracture permeability must be not less than 100 Mdarcy. The change in temperature at the upper part of slice 19 is shown in Fig. 11.

The calculated time for transient state simulation is up to 30,000 years which represent the required time for the model to reach steady state. The result of the simulation shows inhomogeneous distribution of temperature (Fig. 12). The simulation depict recharge in ranges, whereas discharge occurs below the hot spring which the thermal and flow regimes between the underground layers are quite different according to the difference in their permeability. The higher permeability case has significantly more fluid flow below the hot spring. The most important observations obtained from modeling of Hammam Faraun area are the heat source of the hot spring is probably derived from high heat flow and deep circulation controlled by faults associated with the opening of the Red Sea and Gulf of Suez rifts.

Conclusion

There is a clear correlation between the principal areas of current geothermal development and the seismically active boundaries of the moving segments of lithosphere defined by the plate tectonic models of the earth. It would therefore seem logical to concentrate the search for new geothermal resources along the plate boundaries. These indicate potential for development of geothermal resources along the Red Sea and Gulf of Suez coasts. Conceptual and numerical modeling in Hammam Faraun hot spring which represents the hottest spring in Egypt shows that the heat source of the hot spring is probably derived from high heat flow and deep circulation of the underground water. The main sources of this water are from meteoric water and sea water. This water flows upward through faults and fractures associated with the opening of the Red Sea and Gulf of Suez rifts.

References

Barragán RM, Arellano VM, Portugal E, Sandoval F, Barrera VM (2001) Gas equilibrium for the Los Azufres (Michoacán) geothermal reservoir, México, in Proceedings of the 22nd PNOC-EDC Geothermal Conference, March 10–12, Manila, Philippines, pp 81–87

El-Qady G, Ushijima K, El-Sayed A (2000) Delineation of a geothermal reservoir by 2D inversion of resistivity data at Hammam Faraun area, Sinai, Egypt Proc. World Geothermal Congress 2005:1103–1108

El-Nouby MR, Gaber AE (2007) Geothermal studies at Gabel El-Maghara area, North Sinai, Egypt. The Eguptian Society for Envirmental Science, Catrina 2(1):23–32

El Ramly MF (1969) Recent review of investigations on the thermal and mineral springs in the U. A. R. XXIII Int Geol Cong 19:201–213

Fournier RO, Truesdell AH (1973) An empirical Na-K-Ca geothermometer for natural waters. Geochim Cosmochim Acta 37:1255–1275

Gesch DB, Verdin KL, Greenlee SK (1999) New land surface digital elevation model covers the Earth, Eos Trans. AGU 80:69–70

Giggenbach WF (1988) Geothermal solute equilibria. Derivation of Na-K-Ca-Mg geoindicators. Geochim Cosmochim Acta 52:2749–2765

McKenzie DP, Davies D, Molnar P (1970) Plate tectonics of the Red Sea and East Africa. Nature 226:243–248

Meneisy MY (1990) Volcanicity, Chapt 9. In: Said R (ed) Geology of Egypt. Balkema Pub, Rotterdam, Netherlands, pp 157–172

Morgan P, Boulos K, Hennin SF, Elerif AA, El-Sayed AA, Basta NZ, Melek YS (1985) Heat flow in eastern Egypt: the thermal signature of a continental breakup. J Geodyn 4:107–131

Morgan P, Boulos K, Swanberg CA (1983) Regional geothermal exploration in Egypt. EAEG 31:361–376

Moustafa AR, Abdeen AR (1992) Structural setting of the Hammam Faraun block, eastern side of the Suez rift. J Univ Kuwait, Sci 19:291–310

Nicholson K (1993) Geothermal fluids: chemistry and exploration techniques. Springer-Verlag, New York, NY, USA, p 263

Nieva, Nieva R (1987) Developments in geothermal energy in Mexico. Part twelve: a cationic geothermometer for prospecting of geothermal resources. Heat Recov Syst 7:243–258

Palmer MR, Spivack AJ, Edmond JM (1987) Temperature and pH controls over isotopic fractionation during adsorption of boron on marine clay. Geochim Cosmochim Acta 51:2319–2323

Patton TL, Moustafa AR, Nelson RA, Abdine SA (1994) Tectonic evolution and structural setting of the Suez Rift. In: Landon SM (ed) Interior rift basin. American Association Petroleum Geologists Memoir 59:7–55

Said R (1962) The geology of Egypt. Elsevier, Amsterdam, p 377

Sano Y, Nakamura Y, Notsu K, Wakita H (1988) Influence of volcanic eruptions on helium isotope ratios in hydrothermal systems induced by volcanic eruptions. Geochim Gosmochim Acta 52:1305–1308

Sharp IR, Gawthorpe RL, Armstrong B, Underhill JR (2000) Propagation history and passive rotation of mesoscale normal faults: implications for syn-rift stratigraphic development. Basin Res 12:285–306

Sturchio NC, Arehart GB, Sultan M, Sano Y, AboKamar Y, Sayed M (1996) Composition and origin of thermal waters in the Gulf of Suez area, Egypt. Appl Geochem 1 I:471–479

Verma MP (2000) Revised quartz solubility temperature dependence equation along the water-vapor sauration curve, in World Geothermal Congress, Kyushu-Tohoku, Japan, 1927–1932